

# 1 Return Levels of Temperature Extremes in Southern 2 Pakistan

3  
4 Maida Zahid<sup>1</sup>, Richard Blender<sup>1</sup>, Valerio Lucarini<sup>1,2</sup> and Maria Caterina Bramati<sup>3</sup>

- 5 1. Meteorological Institute, University of Hamburg, Hamburg Germany  
6 2. Department of Mathematics and Statistics, University of Reading, Reading, UK  
7 3. Department of Statistical Science, Cornell University, New York, United States

8  
9 *Correspondence to:* Maida Zahid (maida.zahid@uni-hamburg.de)

10  
11 **Abstract.** Southern Pakistan (Sindh) is one of the hottest regions in the world and is highly vulnerable to  
12 temperature extremes. In order to improve rural and urban planning, it is useful to gather information about  
13 the recurrence of temperature extremes. In this work, return levels of the daily maximum temperature  $T_{max}$   
14 are estimated, as well as the daily maximum wet-bulb temperature  $TW_{max}$  extremes. We adopt the Peaks over  
15 threshold (POT) method, which has not yet been used for similar studies in this region. Two main datasets  
16 are analyzed: temperatures observed in nine meteorological stations in southern Pakistan from 1980 to 2013,  
17 and the ERA Interim (ECMWF re-analysis) data for the nearest corresponding locations. The analysis  
18 provides the 2, 5, 10, 25, 50 and 100-year Return Levels (RLs) of temperature extremes. The 90% quantile is  
19 found to be a suitable threshold for all stations. We find that the RLs of the observed  $T_{max}$  are above 50°C in  
20 northern stations, and above 45°C in the southern stations. The RLs of the observed  $TW_{max}$  exceed 35°C in  
21 the region, which is considered as a limit of survivability. The RLs estimated from the ERA Interim data are  
22 lower by 3°C to 5°C than the RLs assessed for the nine meteorological stations. A simple bias correction  
23 applied to ERA Interim data improves the RLs remarkably, yet discrepancies are still present. The results  
24 have potential implications for the risk assessment of extreme temperatures in Sindh.

25  
26 **Key words**

27  
28 Extreme temperature, return levels, peak over threshold, Generalized Pareto Distribution, declustering.

## 29 1 Introduction

30  
31 Extreme maximum temperature events have received much attention in recent years, because of the  
32 associated dangerous impact on the increased risk of mortality (IPCC, 2012). Additionally, climate change  
33 scenarios suggest that in most regions the probability of occurrence of extremely high temperature is very  
34 likely to increase in the future (Sheridan and Allen, 2015). An example of the potential impact of raising  
35 maximum temperatures is the recent heat wave in southern Pakistan (Sindh), which occurred between June  
36 17<sup>th</sup> and June 24<sup>th</sup> 2015 and broke all the records with a death toll of 1400 people, and over 14000 people  
37 hospitalized. The temperatures in different cities of the Sindh region were in the range of 45°C - 49°C during  
38 the event (Imtiaz and Rehman, 2015). Karachi had the highest number of fatalities (1200 people  
39 approximately). The Pakistan Meteorological department issued a technical report stating a very high heat  
40 index (measuring the heat stress on humans due to high temperature and relative humidity) during this heat  
41 wave (Chaudhry et al., 2015).

42  
43 In summer, Sindh becomes very hot and with the arrival of a monsoon the humidity increases in the region

44 (Chaudhry and Rasul, 2004). The extremely hot and humid conditions can have lethal effects, and can impact  
45 the overall human habitability of a region (Pal and Eltahir 2015). The human body generally maintains the  
46 temperature around 37°C. However, the human skin regulates at or below 35°C to release heat (Sherwood  
47 and Huber, 2010). Under combined high temperatures and high levels of moisture content in the atmosphere,  
48 the human body cannot maintain the skin temperature below 35°C and can develop ailments like  
49 hyperthermia, heat strokes and cardiovascular problems. Hyperthermia is a condition where extremely high  
50 body temperature is reached, resulting from the inability of the body to get rid of the excess heat.  
51 Hyperthermia can occur even in the fittest human beings, if exposed for at least six hours to an environment  
52 where wet-bulb temperature is greater than 35°C.

53  
54 This study devotes special attention to Sindh (23.5° N – 28.5° N and 66.5°E - 71.1°E) because of its exposure  
55 to the intense temperature extremes recently (Zahid and Rasul, 2012). It is bounded on the west by the  
56 Kirthar Mountains, to the north by the Punjab plains, on the east by the Thar desert and to the south by the  
57 Arabian Sea (Indian Ocean), while in the center there is a fertile land around the Indus river. Cotton, wheat,  
58 sugar cane, rice, wheat and gram crops are cultivated near banks of the Indus River (Chaudhry and Rasul,  
59 2004). Cotton is the cash crop of the country. High population density, limited resources, poor infrastructure  
60 and high dependence of the local agriculture on climatic factors, mark this region as highly vulnerable to the  
61 impacts of climate change. The Intergovernmental Panel on Climate Change (IPCC) scenarios estimates for  
62 this region an increase in the temperature of the order of 4°C by the end of 2100. This may significantly  
63 reduce crop yields, and cause huge economic losses to the country (Islam et al., 2009; Rasul et al., 2012;  
64 IPCC, 2012, 2014). Furthermore, the risks of heat strokes, cardiac arrest, high fever, diarrhea, cholera and  
65 vector borne diseases might increase.

66  
67 Extreme value theory (EVT) provides the statistical basis for increasingly widespread quantitative  
68 investigations of extremes in climate studies (Coles, 2001, Zhang et al., 2004; Brown et al., 2008; Faranda et  
69 al., 2011; Acero et al., 2014). The peaks over threshold (POT) approach aims at describing the distribution of  
70 the exceedances of the stochastic variable of interest above a threshold. Under very general conditions, the  
71 exceedances are asymptotically distributed according to the Generalized Pareto Distribution (GPD). GPD has  
72 remarkable properties of universality when the asymptotic behavior is considered (Lucarini et al., 2016),  
73 while one can expect that the threshold level above which the asymptotic behavior is achieved depends on  
74 the characteristics of the analyzed time series. In particular, when looking at spatial fields, the threshold level  
75 depends on the geographical location.

76  
77 In this study, we have chosen to analyze the temperature extremes in the Sindh region taking the point of  
78 view of threshold exceedances associated to the GPD family of distributions, because the statistical inference  
79 provided by the POT method provides a more efficient use of data and has better properties of convergence  
80 when finite datasets are considered with respect to alternative methods for the analysis of extremes, such as  
81 the block maxima method, which is used to fit the observed data to the generalized extreme value (GEV)  
82 distribution (Lucarini et al., 2016). Additionally, we are here interested in investigating the actual tails of the  
83 distributions and not the statistics of e.g. yearly maxima, the POT approach is indeed more appropriate.  
84 While the POT method has been applied for studying temperature extremes in different regions of the world

85 (Burgueño et al., 2002; Nogaj et al., 2006; Coelho et al., 2007; Ghil et al., 2011), to our knowledge, it has  
86 never been used to analyze the statistics of temperature extremes in Sindh. Thanks to the properties of  
87 universality of the GPD distribution (Lucarini et al. 2016), the POT approach can in principle provide  
88 reliable estimates of return periods and the return levels also for time ranges longer than what is actually  
89 observed. This information and this predictive power can be beneficial for policy makers and other  
90 stakeholders. Since, it is exactly the kind of information planners need when, e.g., designing infrastructures  
91 that are deemed to last a very long time. Note that commonly used, more empirical approaches to the study  
92 of extremes, as those more used for assessing the ‘moderate extremes’ (IPCC, 2012), do not have any  
93 property of universality and might have weak predictive power.

94  
95 It is useful to consider two indicators of extremely hot conditions: (1) temperature extremes  $T_{max}$ , and (2)  
96 Wet-bulb temperature extremes  $TW_{max}$ . Therefore, we estimate the return levels of  $T_{max}$  and  $TW_{max}$  over  
97 different return periods during summer (May-September) in Sindh. We apply the POT method on the  
98 observational data of the nine weather stations provided by Pakistan Meteorological Department, and the  
99 ERA Interim re-analysis data of European Center for Medium range Weather Forecast (ECMWF) model for  
100 the corresponding grid points from 1980 to 2013. ERA Interim re-analysis data are generally very good at  
101 replicating also trends in temperature percentile (Cornes and Jones, 2013). Nonetheless, it is in principle not  
102 obvious that ERA Interim data can simulate well meteorological extremes, as reanalysis are constructed in  
103 such a way that typical conditions are well reproduced. This is why we look at how well ERA Interim data  
104 performs in the target area against observations. If the ERA Interim dataset characterizes well the extremes,  
105 it could be an option for the regions within Sindh where no observational data is available. Furthermore, a  
106 standard bias correction is applied on the ERA Interim data to assess whether removing the bias in the bulk  
107 of the statistics improves substantially representation of the return levels of extremes. Given the shortness of  
108 the datasets, as we will show later, it is appropriate to analyze the extremes without taking into  
109 considerations possible long-term trends (Frei and Schär, 2001); see also the discussion in Felici et al.  
110 (2007). The provision of POT-based information on stationary extremes is already quite relevant in terms of  
111 impacts for the public and private sector as it fills a big data gap in Sindh. A possibility for investigating time  
112 dependency in the temperature extremes comes for considering the centennial NCEP reanalysis (Compo et  
113 al., 2011) and using suitable bias correction procedures. Such an analysis is not performed at this stage as we  
114 focus on observational data.

115  
116 The paper is organized as follows. In Section 2 we present the datasets we study and the statistical methods  
117 we use for assessing the properties of extremes. In Section 3 we show and discuss the main results. In  
118 Section 4 we make a summary of the main findings and present our conclusions and perspectives for future  
119 investigations.

## 120 **2. Data and Methodology**

### 121 **2.1 Meteorological station data**

122  
123 The daily maximum temperature and relative humidity data recorded at nine meteorological stations in Sindh  
124 from 1980 to 2013 are provided by the Pakistan Meteorological Department (see Table 1). We select nine

125 stations, which contain a negligible amount of missing values after 1980, and are suitable for the POT  
126 analysis (Figure 1). An additional criterion is that only those stations are chosen where no changes occurred  
127 in measuring instruments during the last 33 years (Brunetti et al., 2006). None of the station data shows gaps  
128 with duration longer than two days, which are treated by replacing the missing value with the average of the  
129 two previous values.

130  
131 The temperature data are discretized unevenly with intervals up to 1 degree Celsius. Deidda and Puliga  
132 (2006) proposed a Monte Carlo approach for addressing this issue. They showed that finite resolution in  
133 precipitation data affects the convergence of parameter estimation in the extreme value analysis. They  
134 suggested generating many synthetic datasets by adding numerical noise to the original data, and then  
135 providing the best estimate of the parameters of the extreme value distributions by averaging over all the best  
136 fits obtained in each synthetic dataset. Following their suggestion, we produce high-resolution data to  
137 compensate the effect of discretization and thus to improve the convergence of the estimator. In order to  
138 convert the temperature readings to higher resolution, we add a uniform random variable in the interval  $[-0.5,$   
139  $0.5]$ . The main property of this noise is that  $round(T+r) = T$ , where  $T$  is the temperature with 1-degree  
140 resolution and ‘*round*’ is the numerical function, which maps the interval  $[T-0.5, T+0.5]$  to  $T$ . Thus, adding  
141 the noise does not perturb the information content of the observations. This procedure is applied to all  
142 temperature data, irrespective of the actual resolution, and replicated 100 times using a Monte Carlo  
143 approach. For each synthetic dataset, we perform the statistical best fit described later in the paper and then  
144 average the results. We check the influence of this noise parameterization and find no significant bias in the  
145 return level estimates. The advantage of adding a noise is to avoid the spurious statistical effects associated  
146 to the presence of discrete values assigned to the temperature readings. Using the described bootstrap method  
147 we reduce such problem without biasing the data.  
148

## 149 **2.2 ERA Interim re-analysis data**

150  
151 The gridded daily maximum temperature and relative humidity data of ERA Interim re-analysis is obtained  
152 from the ECMWF Public Datasets web interface (<http://apps.ecmwf.int/datasets/>). The ERA Interim is  
153 generated by the European Center for Medium range Weather Forecast (ECMWF) model with resolution  
154  $0.75^\circ \times 0.75^\circ$  (Dee et al., 2011). The gridded data are then extracted at the closest grid points of all stations,  
155 for the period 1980-2013 (Figure 1). The latitude and longitude of the ERA Interim stations are displayed in  
156 Table 1.

157  
158 The extreme temperatures analysis is restricted to the summer season (May-September) over a period of 33  
159 years. We have tested the datasets by applying the Mann-Kendall test; the results show that trends are not  
160 significant in such a short time interval. One of the main requirements for performing the POT analysis is  
161 assuming the stationarity of the time series. Therefore, as in Bramati et al. (2014), the Augmented Dickey  
162 Fuller (ADF) test of stationarity is performed on all time series (Dickey and Fuller, 1979). In all cases we  
163 find no sign of long-term correlations in the data. Short-term correlations (daily time scale) typically lead to



164 clusters of extreme values and are studied by computing the extremal index  $\theta$  in all time series and treated  
165 using the associated standard declustering technique (see more details in Section 2.4).  
166

### 167 **2.3 Wet-bulb temperature calculations**

168  
169 The wet-bulb temperature measures the heat stress better than other existing heat indices, because it  
170 establishes the clear thermodynamic limit on heat transfer that cannot be overcome by adaptations like  
171 clothing, activity and acclimatization (Pal and Eltahir, 2015; Sherwood and Huber, 2010). Here, we use an  
172 empirical equation developed by Stull (2011) to measure the wet-bulb temperature.  
173

$$174 \quad TW = T \operatorname{atan}(\alpha_1 \sqrt{RH + \alpha_2}) + \operatorname{atan}(T + RH) - \operatorname{atan}(RH + \alpha_3) + \alpha_4 (RH)^{\frac{3}{2}} \operatorname{atan}(\alpha_5 RH) -$$
$$175 \quad \alpha_6 \tag{1}$$

176  
177  
178

179 where  $TW$  is the wet-bulb temperature [ $^{\circ}\text{C}$ ],  $T$  is the temperature [ $^{\circ}\text{C}$ ], and  $RH$  is the relative humidity [%].  
180 This relationship is based on an empirical fit, as in Stull (2011), where the coefficient values are  $\alpha_1 =$   
181  $0.151977$ ,  $\alpha_2 = 8.313659$ ,  $\alpha_3 = -1.676331$ ,  $\alpha_4 = 0.00391838$ ,  $\alpha_5 = 0.023101$ , and  $\alpha_6 = 4.686035$ . Equation (1)  
182 covers a wide range of relative humidity and air temperatures with an accuracy of  $0.3^{\circ}\text{C}$ .  
183

### 184 **2.4 Peaks over Threshold**

185  
186 In order to determine the return levels of extreme maximum temperatures and maximum wet-bulb  
187 temperatures, the peaks over threshold (POT) approach is applied to the data obtained from the  
188 meteorological stations in Sindh, and from the ERA Interim archive.  
189

190 Multi-occurrence is an important characteristic of extreme climatic events and is referred to as clustering.  
191 Clusters are consecutive occurrences of above threshold events. It is important to post process the clustered  
192 extremes in order to take into account the assumption of weak short time correlation between extreme events,  
193 which is crucial for our statistical analysis. We have treated the clusters using the concept of Extremal Index  
194 (EI) (see Newell, 1964, Loynes, 1965, O'Brien, 1974, Leadbetter, 1983, Smith, 1989, Davison and Smith,  
195 1990). The Extremal Index  $\theta$  measures the degree of clustering of extremes. It ranges between 0 and 1, ( $\theta = 0$   
196 means strong clustering and dependence,  $\theta = 1$  absence of clusters and independence). Leadbetter (1983)  
197 interprets  $1/\theta$  as the mean number of exceedances in a cluster.  
198

199 The extremal index  $\theta$  can be estimated in two different ways. Here, we apply the 'intervals estimator'  
200 automatic declustering by Ferro and Segers (2003). A positive aspect of this method is that it avoids the  
201 subjective choice of cluster parameters. The main ingredient is the use of an asymptotic result for the times  
202 between threshold exceedances. The exceedance times are split into two types, a set of vanishing intra-  
203 exceedance times within the clusters, and an exponentially distributed set of inter-exceedance times between  
204 clusters. The method is iterative, starting with largest return times and stops when a limit for the inter-

205 exceedance times is reached. The standard errors of the estimated parameters is obtained by a bootstrap  
 206 procedure. In this study, once we select appropriate value for the threshold (see below) the extremal index  
 207 value is  $\leq 0.5$  in all the considered time series. Therefore, it is necessary to decluster the extremes by  
 208 choosing the largest event in each cluster, before fitting it to the GPD.

209  
 210 As mentioned before, we use as statistical model for the exceedances over threshold the Generalized Pareto  
 211 Distribution (GPD), which is characterized by two parameters, the shape  $\xi$  and the scale  $\sigma$ . The GPD for  
 212 exceedances  $x - u$  of a random variable  $x$  reads as

$$213 \quad G(x) = 1 - \left[ 1 + \xi \left( \frac{x - u}{\sigma} \right) \right]^{-\frac{1}{\xi}} \quad (x > u, \xi \neq 0) \quad (2)$$

214  
 215 where  $u$  is the threshold. The shape parameter  $\xi$  determines the tail behavior while the scale parameter  $\sigma$   
 216 measures the variability. For a negative shape parameter,  $\xi < 0$ , the distribution is bounded (Weibull  
 217 distribution), for vanishing shape parameter,  $\xi = 0$ , the distribution is exponential, and for a positive shape  
 218 parameter,  $\xi > 0$ , the distribution has no upper bound (Pareto distribution).

219  
 220 In particular, for a negative shape parameters  $\xi < 0$  the GPD has the upper bound

$$221 \quad A_{max} = u - \sigma / \xi \quad (3)$$

$$222 \quad G(x) = 0 \quad (x > A_{max}, \xi < 0)$$

223  
 224 where  $A_{max}$  is an absolute maximum (Lucarini et al., 2014). In general, the best estimate for the two  
 225 parameters shape  $\xi$  and scale  $\sigma$  depend on the threshold  $u$  (Coles, 2001). The choice of the optimal threshold  
 226 for performing statistical inference from a time series is crucial. Choosing a very large value for  $u$  reduces  
 227 the number of exceedances to a few values, inflating the variance of the estimators, so that the analysis is  
 228 unlikely to yield any useful results. On the other hand, choosing a too small value for  $u$  would violate the  
 229 asymptotic nature of the model, with a possible biased estimation and wrong model selection (Coles, 2001),  
 230 see details later in Section 3.1. The shape  $\xi$ , the scale  $\sigma$  and the return levels are estimated using the  
 231 Maximum Likelihood Estimator (MLE) using the R software (R Development core team 2015), which also  
 232 provides an estimate of the standard error of the estimates.

233  
 234 Additionally, we wish to investigate the  $N$  - years return levels  $x_N$ , which are exceeded on the time scale of  
 235  $N$  years (Coles, 2001) and can be expressed as

$$236 \quad x_N = u + \frac{\sigma}{\xi} \left[ (N n_y \zeta_u)^\xi - 1 \right] \quad (4)$$

237  
 238 where  $N$  represents the return period in years,  $n_y$  is the number of observations per year,  $\zeta_u$  is the probability  
 239 of an individual observation exceeding the threshold  $u$ , the shape parameter is  $\xi$  and the scale parameter is  
 240  $\sigma$ .

245 **2.5. Bias Correction Method**

246  
247 A simple bias correction is applied to each ERA Interim time series through a rescaling that adjust the first  
248 two moments (mean and variance) to the sample moments calculated for the corresponding observations.  
249 Therefore, the bias correction is applied to the entire time series and it is not tailored to the extreme events  
250 only. The idea is to check whether by adjusting the properties of the bulk of the statistics we improve the  
251 skill of the ERA Interim dataset considerably in describing extreme events. The bias corrected ERA Interim  
252 time series  $x$  is expressed as  
253

$$x = \bar{z} + \frac{y_{ERA} - \bar{y}}{\sigma_y} \sigma_z \quad (5)$$

254  
255  
256  
257 where  $y_{ERA}$  is the ERA Interim time series,  $\bar{y}$  and  $\sigma_y$  its mean and standard deviation, whereas  $\bar{z}$  and  
258  $\sigma_z$  are the mean and standard deviation of the meteorological station temperatures. The properties of  
259 extremes are commonly assumed to be closely controlled by the first two moments of the underlying  
260 distribution - e.g. the IPCC (2012) relates changes in the properties of extremes to changes in the mean and  
261 in the standard deviation of the underlying distributions - EVT clarifies that, in fact, only a loose link exists  
262 between true extremes and the bulk of the events. Note that the proposed method of bias corrections has no  
263 impact on the estimates of the shape parameter, while it affects the scale and location parameters, thus  
264 impacting at any rate the return levels.

265 **3. Results and Discussion**

266 **3.1 Threshold Selection**

267  
268 The threshold selection is the first step in a POT analysis. One needs to test whether the asymptotic regime is  
269 reached, i.e. whether one is choosing true extremes. It must be noted that EVT does not predict where (in  
270 terms of quantiles) one should expect the asymptotic regime to start. This can be investigated by checking  
271 whether the best fits of the shape parameter  $\xi$  and the modified scale parameter  $\sigma^* = \sigma_u - \xi u$  are stable with  
272 respect to increases in the chosen value of  $u$  (Sacrotto and MacDonald, 2012). The optimal threshold  $u$  is  
273 selected as the lowest value where the two parameters are invariant in order to reach the asymptotic limit  
274 (Coles, 2001 and Furrer et al., 2010). This choice allows for having as many data as possible for performing  
275 the statistical inference, thus having lower variance for the estimators of the parameters. Figure 2 shows the  
276 parameter stability plots of the  $T_{max}$  reading for Karachi, as an example to explain the threshold selection  
277 procedure.  
278

279 In addition to diagnostic plots of the modified scale parameter  $\sigma^*$  and the shape parameter  $\xi$ , the mean  
280 residual life plot is used to select the appropriate threshold for the POT analysis (Davison and Smith, 1990).  
281 The idea is to select the lowest value of the threshold when the plot is approximately linear. In the case of the  
282 Karachi data for  $T_{max}$ , the plot appears to be linear and stable for  $u = 36^\circ\text{C}$ , indicating  $u = 36$  as the most

283 suitable threshold for the POT analysis (Figure 3). We observe that the 90% quantile is an appropriate  
284 threshold for all the station data, as well as the ERA interim datasets, and for both  $T_{max}$ , and  $TW_{max}$ .  
285

### 286 3.2 GPD Fit

287  
288 The goodness of fit is evaluated by Quantile-Quantile (Q-Q) plots and hypothesis testing. The Q-Q plot  
289 analysis is performed for the stations observed, the ERA Interim, the bias corrected ERA Interim daily  $T_{max}$   
290 and  $TW_{max}$ . The Q-Q plots of the observed  $T_{max}$  show that the GPD fits well in most stations. However, in a  
291 few stations like Jacobabad, Mohenjo-daro, Padidan and Chhor the empirical values show slight deviation  
292 from the modeled values. In spite of minor deviations at some stations, still most of the exceedances are well  
293 fitted by the model. The Q-Q plots of the observed  $TW_{max}$  also fits well to the model in all stations.  
294

295 The Q-Q plots of the empirical ERA Interim  $T_{max}$  and  $TW_{max}$  data reveals substantial differences with  
296 respect to the corresponding GPD fits. The empirical values of the higher quantiles are deviating from the  
297 theoretical quantiles in all stations. However, if the higher quantiles are disregarded, then stations like  
298 Jacobabad, Mohenjo-daro, Rohri, Padidan, Nawabshah, Chhor, and Badin fits very well with the model. The  
299 Q-Q plots of the bias corrected ERA Interim  $T_{max}$ , and  $TW_{max}$  show better results than the ERA Interim. We  
300 notice that the  $T_{max}$  of the ERA Interim and bias corrected ERA Interim fits better than the  $TW_{max}$  if the  
301 highest quantiles are ignored, indicating the bias procedure is, as expected, unable to treat correctly the  
302 statistics of the largest events.  
303

304 In order to assess the goodness-of-fit, we apply the Kolmogorov-Smirnov (K-S) test and Anderson-Darling  
305 (A-D) test to the data of meteorological stations, ERA Interim, bias corrected ERA Interim  $T_{max}$  and  $TW_{max}$ .  
306 The p-values indicate a good performance of the fit procedure. Table 2 shows the results of the K-S and A-D  
307 statistics of the  $T_{max}$  and  $TW_{max}$  in all the data sets.  
308

### 309 3.3 Parameter Estimates

310  
311 Here, we analyze the shape parameter  $\xi$ , the scale parameter  $\sigma$ , and threshold  $u$  for all considered datasets.  
312 The standard errors of the shape  $\xi$  and the scale  $\sigma$  parameters are given in Table 3. The spatial distribution of  
313 the shape parameter  $\xi$  and the scale parameter  $\sigma$  of the GPD in Sindh are shown in Figure 4. The shape  
314 parameters  $\xi$  are negative in all datasets at all stations. This is hardly surprising, as meteorological and  
315 physical processes make sure that the temperature cannot grow locally without control. One finds a certain  
316 degree of variability across stations in the estimated value of the shape parameter. In the case of the observed  
317  $T_{max}$  one obtains for  $\xi$  estimates ranging between -0.418 and -0.223, while for  $TW_{max}$  the range is between -  
318 0.323 and -0.177, so that values slightly closer to zero are found, thus allowing for larger excursions towards  
319 very high values with respect to the case of the extremes of the actual temperature. When looking at the bias  
320 corrected ERA Interim data, the range of values for the shape parameter of  $T_{max}$  ( $TW_{max}$ ) is between -0.305 to  
321 -0.002 (-0.18 and -0.01). While there is a good match in the spatial patterns of the estimates for the  
322 observative vs ERA Interim datasets, the presence of values much closer to zero in the second case suggests

323 the presence of some inadequacies in the representation of extremes in the reanalysis. This is not entirely  
324 unexpected, as reanalysis are constructed in such a way that typical conditions are well reproduced. Note that  
325 our simple bias correction procedure, while not impacting the estimates of the shape parameters, allows for  
326 improving the estimates of the return levels, as discussed below.

327  
328 The scale parameters  $\sigma$  measures the variability of the GPD distributions. The highest values of the scale  
329 parameters  $\sigma$  of  $T_{max}$  and  $TW_{max}$  are observed at stations such as Jacobabad, Padidan, Karachi, Hyderabad  
330 and Chhor in all datasets. This indicates that the variability of temperature extremes is higher at these  
331 stations, and one can expect higher return values of  $T_{max}$  and  $TW_{max}$  here having similar shape parameter  
332 and same threshold according to Equation 4. The scale parameters  $\sigma$  of the observed  $T_{max}$  range from 2.08 to  
333 2.76, and the  $TW_{max}$  are in 1.86 to 2.76. In the ERA Interim analysis, the scale parameter  $\sigma$  of  $T_{max}$  is  
334 between 1.00 - 1.95, and  $TW_{max}$  in 0.74 -1.75. We observe a difference in the scale parameters of both the  
335 observed, ERA Interim  $T_{max}$  and  $TW_{max}$ . We find that, unsurprisingly, the scale parameters of the bias  
336 corrected ERA Interim data are much closer to those estimated for  $T_{max}$  and  $TW_{max}$  using the station data. In  
337 the bias corrected ERA Interim  $T_{max}$  the scale parameters  $\sigma$  are in 1.50 - 2.75, while for  $TW_{max}$  are in a range  
338 1.40 – 2.40 (Figure 4). All the temperature scale parameters are in degree Celsius.

339

### 340 **3.4 Absolute Maxima**

341

342 Once the shape parameters  $\xi$ , the scale parameters  $\sigma$ , and the thresholds  $u$  are determined, it is possible to  
343 compute the theoretical absolute maxima using Eq. (3) (Section 2.4). Theoretical absolute maxima can be  
344 compared with the observed ones for each station to better understand whether our fits are in agreement with  
345 the observed data. The daily maximum temperature  $T_{max}$  and the maximum wet-bulb temperature  $TW_{max}$   
346 (station data, the ERA Interim, and the bias corrected ERA Interim) have negative shape parameters  $\xi$  at all  
347 stations. This means that according to Eq. (2) in section 2.4, the probability distribution function (pdf) is  
348 bounded by the maximum values. These maximum values are the theoretical upper limits predicted by the  
349 GPD fit. The analysis shows that the observed absolute maxima  $T_{max}$  and  $TW_{max}$  at all stations of the three  
350 data sets are below the theoretical absolute maximum, as expected (Figure 5). This gives us confidence on  
351 the quality of our fit. The following piece of information can also be derived: assume that one observes in the  
352 future an extreme event larger than the maximum inferred in the present dataset; this may suggest some non-  
353 stationarity in the most recent portion of the dataset.

354

### 355 **3.5 Return Levels**

356

357 The return levels (RLs) are computed considering various return periods (2, 5, 10, 20, 50, 100-year). As  
358 remarked above, using a statistical approach based on the universality of EVT, we are able to extrapolate the  
359 results for time horizons longer than the one for which observations are taken. Clearly, uncertainties grow  
360 when longer time horizons are considered. The return level plots of the stations observed, the ERA Interim,  
361 the bias corrected ERA Interim daily maximum temperature  $T_{max}$  and daily maximum wet–bulb temperature  
362  $TW_{max}$  are displayed in Figures 6 and 7. The values of the RLs follow the north-south gradient of the climatic

363 mean temperatures. The northern part of the Sindh (Jacobabad, Mohenjo-daro, Rohri, Padidan, and  
364 Nawabshah) are hotter than the southern part (Hyderabad, Chhor, Karachi, and Badin).

365  
366 The 2, 5, 10, 20, 50, 100-year RLs estimated in Sindh for station observed  $T_{max}$  at time reach over 50°C in  
367 Jacobabad, Mohenjo-daro, Padidan, Nawabshah, and over 45°C in Rohri, Hyderabad, Chhor, Karachi,  
368 Badin. The corresponding ERA Interim  $T_{max}$  return levels are at least 3°C to 5°C lower in all stations, while  
369 having correct representation of the geographical variability of the field. As example, the RLs of 42°C at  
370 Badin has a 3-year return period in the observations  $T_{max}$ , but a 30-year return period in ERA Interim (Figure  
371 6).

372  
373 The RLs of  $TW_{max}$  are above 35°C in all meteorological stations. As for the ERA Interim, the RLs of  $TW_{max}$   
374 are greater than 30°C for all the stations except Karachi, which has RLs less than 30°C. Here, we see again  
375 that the RLs of the ERA Interim  $TW_{max}$  are lower than the RLs of station  $TW_{max}$ . Going again to the Badin  
376 stations, the 4-year return period observed for  $TW_{max}$  is 38°C, while the ERA Interim dataset show the same  
377 RL in a 15-year return period (Figure 7).

378  
379 The bias corrected ERA Interim  $T_{max}$  and  $TW_{max}$ , show some improvements in the RLs at all stations. When  
380 looking at the Nawabshah, Hyderabad, Karachi, and Badin stations, the RLs agree with those obtained from  
381 the station data in the range 5-100 years, while disagreements exist in the range 2-5 years. In the rest of the  
382 stations, the bias corrected data RLs are closer to those of the station data, yet not statistically compatible  
383 with them. When looking at the wet-bulb temperature  $TW_{max}$  analysis, the RLs of the bias corrected ERA  
384 Interim show some overlap with those derived from station observations in Mohenjo-daro, Hyderabad,  
385 Chhor, and while no overlap is found in the other stations. One understands that the proposed simple bias  
386 correction methods improves the quality of the representation of extremes by ERA Interim, but many  
387 discrepancies remain (Figures 6 and 7).

388  
389 We also plot the station and bias corrected ERA Interim  $T_{max}$ , and  $TW_{max}$  return levels spatially for the 5, 10,  
390 25 and 50-year return periods (Figures 8 and 9), as a detailed spatial overview of the temperature extremes  
391 in Sindh might be of interest to the policy makers. The spatial return levels of the station and bias corrected  
392 ERA Interim  $T_{max}$  shows differences in temperature; the hottest stations have the highest return levels. We  
393 notice that for Jacobabad, Mohenjo-daro, Padidan, Nawabshah the return levels are between 50°C-53.6°C  
394 and for Rohri, Hyderabad, Chhor, Karachi, and Badin are between 45°C - 50°C in 5 to 50 years return period  
395 (Figure 8). These extreme temperatures can impact the yields because crops are very sensitive to temperature  
396 variations, and even a rise of one degree Celsius can cause detrimental changes in the phenological stages of  
397 the crops (Hatfield and Preuger, 2015). Every crop has a certain limit to tolerate the temperature. When  
398 temperature exceeds this limit, the crop yield is drastically reduced. Abbas et al., (2017) notices 33%  
399 decrease in major crops of Sindh due to warmer and drier weather. Karachi and Badin are expected to  
400 decrease rice cultivation, hatching of fisheries, and mangroves forest surrounding these cities. Furthermore,  
401 temperature extremes can have serious threat to cotton, wheat, and rice yields in Rohri and Mohenjo-daro  
402 areas due to increased crop water requirements.

403  
404 In summer, the temperature and humidity increase to an extent that there are high chances of a rapid pests  
405 spread in the crops. Temperature extremes not just directly impact the quantity and quality of grains, but can  
406 also be a reason of urban flooding affecting the agriculture lands (Luo et al., 2015). Sindh produces cotton,  
407 wheat, rice, mango, banana, and dates, so a correct estimate of temperature extremes is very important.

408  
409 The spatial return levels of station and bias corrected ERA Interim  $TW_{max}$  for the 5, 10, 25 and 50-year  
410 return periods show highest return level greater than  $35^{\circ}\text{C}$  at all stations (Figure 9). This is very serious for  
411 the human health due to the working day hours of population in agriculture farms, building construction, and  
412 port activities. Karachi and Badin being closet to the coast are at the highest risk of temperature extremes.  
413 Thus, an immediate plan for adaptations is needed in Sindh to deal with such a hazard. The high values of  
414  $TW_{max}$  also indicate high levels of humidity in the region during summer, which is also proved by Kalim  
415 and Shouting, (2012), and Freychet et al. (2015).

#### 416 **4. Summary and Conclusion**

417  
418 The main objective of this study is the assessment of the return levels of the extreme daily maximum  
419 temperatures  $T_{max}$  and wet-bulb temperatures  $TW_{max}$  in southern Pakistan (Sindh). In addition, the  
420 performance of the ERA Interim  $TW_{max}$  is compared to the weather station  $TW_{max}$  to assess its ability to  
421 estimate temperature extremes in Sindh. Moreover, a simple bias correction is applied to the ERA Interim  
422 data to see whether correcting the first two moments of its statistics helps in improving its performance in  
423 representing temperature extremes.

424  
425 The POT method is applied to the daily maximum temperature ( $T_{max}$ ) and wet-bulb temperature ( $TW_{max}$ ) data  
426 of nine stations and to the corresponding nearest ERA Interim temperature data. After testing the asymptotic  
427 statistical properties, the 90% quantile is found to be appropriate threshold choice for all datasets. The Q-Q  
428 plots are used to assess the GPD fit, which results to be acceptable for both  $T_{max}$  and  $TW_{max}$  station data for  
429 all three datasets. However, the bias corrected ERA Interim data shows improved GPD fits than the ERA  
430 Interim data. The shape parameters  $\xi$  is in general negative at all stations. The scale parameters  $\sigma$  show high  
431 values in Jacobabad, Padidan, Karachi, Hyderabad and Chhor indicating higher variability of temperature  
432 extremes in these regions. The return levels (RLs) of  $T_{max}$  and  $TW_{max}$  are estimated for the 2, 5, 10, 25, 50,  
433 100-year return periods in all datasets. The RLs of  $T_{max}$  estimated using the meteorological station  
434 temperatures are greater than  $50^{\circ}\text{C}$  in Jacobabad, Mohenjo-daro, Padidan, Nawabshah, and greater than  $45^{\circ}\text{C}$   
435 in Rohri, Hyderabad, Chhor, Karachi and Badin. While the RLs of  $TW_{max}$  in station data are larger than  $35^{\circ}\text{C}$   
436 in the entire Sindh, when using ERA Interim temperatures, they are estimated as greater than  $45^{\circ}\text{C}$  in  
437 Northern Sindh and greater than  $40^{\circ}\text{C}$  in southern Sindh.

438  
439 Our results predict extremely high values of  $T_{max}$  and  $TW_{max}$  in the region. The  $T_{max}$  extremes contribute to  
440 an increase rate of evaporation, which in turn may intensify the hydrological cycle causing precipitation  
441 events and flooding (Cheema et al., 2012, Luo et al., 2015). Additionally, crops variety needs to be changed

442 under such a hot climate to avoid the risks of temperature extremes. The extremes of daily maximum wet-  
443 bulb temperature  $TW_{max}$  are estimated as above the human survivability threshold  $35^{\circ}\text{C}$  throughout the  
444 region, so the risk of hyperthermia is very high here. The most vulnerable people are those who are involved  
445 in the everyday outdoor activities like farming, fishing, building construction, athletes, elderly and infants  
446 can have heat strokes, dehydration etc. The human habitability in such a warm region is already at risk and  
447 one can expect that these issues will be worse in future climate conditions.

448  
449 We found that the RLs of station and ERA interim showed differences between  $3^{\circ}\text{C}$  and  $5^{\circ}\text{C}$  for both shorter  
450 and longer return periods due to the minor variations in the shape and scale parameters. Although the ERA  
451 Interim dataset does not capture well the magnitude of the extremes, still it provides a good representation of  
452 their spatial fields. The biases between the station and the ERA Interim data are rather relevant when one  
453 wishes to address the impact of hot climatic extremes to human life and to active crop production in the  
454 region. It would be of primary importance to understand the physical reasons behind such inconsistencies,  
455 which makes it hard to use reasonably ERA without bias correction. Clearly, they might result either from a  
456 misrepresentation of local processes dominated by near surface processes (namely, heat and water fluxes), or  
457 from an inadequacy of the re-analysis in reproducing synoptic and sub-synoptic conditions responsible for  
458 extremely hot and humid conditions. This matter is surely worth investigating but is well beyond the scope  
459 of this paper.

460  
461 We applied a simple bias correction i.e. adjusting the mean and standard deviation to ERA Interim  $T_{max}$  and  
462  $TW_{max}$  data to check the improvements in return levels. We noticed that the bias corrected ERA Interim  $T_{max}$   
463 and  $TW_{max}$  gives the return levels closer to the meteorological stations observed ones than the original ERA  
464 Interim return levels at all stations. Although the bias corrected ERA Interim shows a good correspondence  
465 with the meteorological station data, yet statistically significant differences remain in most cases. Therefore,  
466 one must use more advanced bias correction method for analyzing extremes precisely. We propose to repeat  
467 this analysis in GCMs (CMIP5, CMIP6) and RCMs (CORDEX) to study the properties of extremes. All  
468 models use re-analysis as input, and generate information of extremes, which involves biases that if not  
469 corrected, can lead to significant errors in prediction of present and future extremes. Therefore, in order to  
470 reduce the uncertainties in impact assessment, it is necessary to improve the re-analysis before using it in  
471 GCMs and RCMs.

472  
473 The results have practical implications for assessing the risk of extreme temperature events in Sindh. All the  
474 results are placed in a web-tool SindheX [[www.sindhhex.org](http://www.sindhhex.org)] that will be freely available online soon after  
475 the publication of this paper. The maps and graphs are prepared to guide the local administrations to  
476 prioritize the regions in terms of adaptations like preparation of baseline contingency plans for dealing with  
477 strong heat waves based on the current climatology. Such measures are not yet present in the territory and  
478 lead to many casualties each year. Our results will not only contributes to the regional planning, but can also  
479 be useful for the ongoing EU projects (SUCCESS, CSCCC), World Bank project (Sindh Resilience Project)  
480 and mega construction projects like China-Pakistan Economic Corridor (CPEC).

481



482 **Acknowledgements**

483  
484 We would like to thank Climate KIC, for funding this research. This publication is a part of a Climate KIC  
485 project “Extreme Events in Pakistan: Physical processes and impacts of changing climate”, which belongs to  
486 the adaptation services platform of the Climate KIC. Thanks to Pakistan Meteorological Department (PMD)  
487 and the European Center for Medium range Weather Forecast (ECMWF) for providing the datasets. The R  
488 development core team (2015) is acknowledged for providing statistics packages. We would like to thank the  
489 DFG Cluster of Excellence CliSAP for partially supporting this research activity. We would like to thank the  
490 reviewers, whose constructive criticisms have greatly helped to improve the quality of this paper.

491 **References**

492  
493 Abbas, F., Rehman, I., Adrees, M., Ibrahim, M., Saleem, F., Ali, S., Rizwan, M. and Salik, M. R.: Prevailing  
494 trends of climatic extremes across Indus-Delta of Sindh-Pakistan, *Theor. Appl. Climatol.*,  
495 doi:10.1007/s00704-016-2028-y, 2017.  
496  
497 Acero, F. J., García, J. A., Gallego, M. C., Parey, S. and Dacunha-Castelle, D.: Trends in summer extreme  
498 temperatures over the Iberian Peninsula using nonurban station data, *J. Geophys. Res. Atmos.*,119, 39-53,  
499 doi:10.1002/2013JD020590, 2014.  
500  
501 Bramati, M.C., Tarragoni, C., Davoli, L., Raffi, R., Extreme Rainfall in Coastal Metropolitan Areas of  
502 Central Italy: Rome and Pescara case studies. *Geografia Fisicae Dinamica Quaternaria*, 37, 3-13, 2014.  
503  
504  
505 Brunetti, M., Maugeri, M., Monti, F. and Nanni, T.: Temperature and precipitation variability in Italy in the  
506 last two centuries from homogenized instrumental time series, *J. Climatol.*, 26(3), 345–381,  
507 doi:10.1002/joc.1251, 2006.  
508  
509 Burgueño, A., Lana, X. and Serra, C.: Significant hot and cold events at the Fabra Observatory, Barcelona  
510 (NE Spain), *Theor. Appl. Climatol.*, 71(3), 141-156, doi:10.1007/s007040200001, 2002.  
511  
512 Brunetti, M., Maugeri, M., Monti, F. and Nanni, T.: Temperature and precipitation variability in Italy in the  
513 last two centuries from homogenized instrumental time series, *J. Climatol.*, 26(3), 345–381,  
514 doi:10.1002/joc.1251, 2006.  
515  
516 Brown, S. J., Caesar, J. and Ferro, C. A. T.: Global changes in extreme daily temperature since 1950, *J.*  
517 *Geophys. Res. Atmos.*, 113, D05115 doi:10.1029/2006JD008091, 2008.  
518  
519 Chaudhry, Q.-U.-Z. and Rasul, G.: AGRO-CLIMATIC CLASSIFICATION OF PAKISTAN, *Q. Sci. Vis.*,  
520 9(12), 3–4, 2004.  
521  
522 Chaudhry, Q. Z., Rasul, G., Kamal, A., Ahmad Mangrio, M. and Mahmood, S.: Government of Pakistan  
523 Ministry of Climate Change Technical Report on Karachi Heat wave June 2015.  
524  
525 Cheema S.B., Zaman Q. & Rasul G. Persistent heavy downpour in desert areas of Pakistan in South Asian  
526 Monsoon 2011. *Pak J Meteorol*, 9, (17), 71–84, 2012.  
527  
528  
529 Coles, S.: *An Introduction to Statistical Modeling of Extreme Values*, Springer London, London., 2001.  
530  
531 Coelho, C. A. S., Ferro, C. A. T., Stephenson, D. B. and Steinskog, D. J.: Methods for Exploring Spatial and  
532 Temporal Variability of Extreme Events in Climate Data, *J. Clim.*, 21(10), 2072–2092,  
533 doi:10.1175/2007JCLI1781.1, 2007.  
534  
535 Compo, G.P., J.S. Whitaker, P.D. Sardeshmukh, N. Matsui, R.J. Allan, X. Yin, B.E. Gleason, R.S. Vose, G.  
536 Rutledge, P. Bessemoulin, S. Brönnimann, M. Brunet, R.I. Crouthamel, A.N. Grant, P.Y. Groisman, P.D.  
537 Jones, M. Kruk, A.C. Kruger, G.J. Marshall, M. Maugeri, H.Y. Mok, Ø. Nordli, T.F. Ross, R.M. Trigo, X.L.  
538 Wang, S.D. Woodruff, and S.J. Worley: The Twentieth Century Reanalysis Project. *Quarterly J. Roy.*  
539 *Meteorol. Soc.*, 137, 1-28. <http://dx.doi.org/10.1002/qj.776>, 2011.  
540  
541 Cornes, R. C., and P. D. Jones, How well does the ERAInterim reanalysis replicate trends in extremes of  
542 surface temperature across Europe? *J. Geophys. Res.*, 118, 10 262– 10 276, doi:10.1002/jgrd.50799, 2013.  
543  
544 Davison, A. C. and Smith, R. L.: Models for Exceedances over High Thresholds, *J. R. Stat. Soc. Ser. B*,

545 52(3), 393–442, doi:10.2307/2345667, 1990.

546

547 Dee, D. P., Uppala, S. M., Simmons, A. J., Berrisford, P., Poli, P., Kobayashi, S., Andrae, U., Balmaseda, M.

548 A., Balsamo, G., Bauer, P., Bechtold, P., Beljaars, A. C. M., van de Berg, L., Bidlot, J., Bormann, N., Delsol,

549 C., Dragani, R., Fuentes, M., Geer, A. J., Haimberger, L., Healy, S. B., Hersbach, H., Hólm, E. V., Isaksen,

550 L., Kállberg, P., Köhler, M., Matricardi, M., McNally, A. P., Monge-Sanz, B. M., Morcrette, J. J., Park, B.

551 K., Peubey, C., de Rosnay, P., Tavolato, C., Thépaut, J. N. and Vitart, F.: The ERA-Interim reanalysis:

552 Configuration and performance of the data assimilation system, *Q. J. R. Meteorol. Soc.*, 137: 553–597,

553 doi:10.1002/qj.828, 2011.

554

555 Deidda, R. and Puliga, M.: Sensitivity of goodness-of-fit statistics to rainfall data rounding off, *Phys. Chem.*

556 *Earth*, 31, 1240–1251, doi:10.1016/j.pce.2006.04.041, 2006.

557

558 Dickey, D. A. and Fuller, W. A.: Distribution of the Estimators for Autoregressive Time Series With a Unit

559 Root, *J. Am. Stat. Assoc.*, 74(366), 427, doi:10.2307/2286348, 1979.

560

561 Faranda, D., Lucarini, V., Turchetti, G. and Vaienti, S.: Numerical Convergence of the Block-Maxima

562 Approach to the Generalized Extreme Value Distribution, *J. Stat. Phys.*, doi:10.1007/s10955-011-0234-7,

563 2011.

564

565 Felici, M.; Lucarini, V.; Speranza, A.; Vitolo, R. Extreme value statistics of the total energy in an

566 intermediate-complexity model of the midlatitude atmospheric jet. Part II: trend detection and assessment.

567 *Journal of the Atmospheric Science*, v.64, p.2159-214-75, 2007.

568

569 Ferro, C. A. T. and Segers, J.: Inference for clusters of extreme values, *J. R. Stat. Soc. B*, 65(2), 545–556,

570 2003.

571

572 Frei, C., and C. Schär, Detection probability of trends in rare events: Theory and application to heavy

573 precipitation in the Alpine region. *J. Climate*, 14, 1568–1584, 2001.

574

575 Furrer, E., Katz, R., Walter, M. and Furrer, R.: Statistical modeling of hot spells and heat waves, *Clim. Res.*,

576 43(3), 191–205, doi:10.3354/cr00924, 2010.

577

578 Freychet, N., Hsu, H.-H., Chia, C., and Wu, C.-H., Asian Summer Monsoon in CMIP5 Projections : A Link

579 between the Change in Extreme Precipitation and Monsoon Dynamics. *J. Climate*, pages 1477–1493, 2015.

580

581 Ghil, M., Yiou, P., Hallegatte, S., Malamud, B. D., Naveau, P., Soloviev, A., Friederichs, P., Keilis-Borok,

582 V., Kondrashov, D., Kossobokov, V., Mestre, O., Nicolis, C., Rust, H. W., Shebalin, P., Vrac, M., Witt, A.

583 and Zaliapin, I.: Extreme events: Dynamics, statistics and prediction, *Nonlinear Process. Geophys.*, 18, 295-

584 350, doi:10.5194/npg, 2011.

585

586 Hatfield, J. L. and Prueger, J. H.: Temperature extremes: Effect on plant growth and development, *Weather*

587 *Clim. Extrem.*, 10, 4-10, doi:10.1016/j.wace.2015.08.001, 2015.

588

589 Imtiaz S, Rehman, ZU. 2015. June 25. Death Toll From Heat Wave in Karachi, Pakistan, Hits 1,000. *The*

590 *New York Times* retrieved from [http://www.nytimes.com/2015/06/26/world/asia/karachi-pakistan-heat-wave-](http://www.nytimes.com/2015/06/26/world/asia/karachi-pakistan-heat-wave-deaths.html?_r=0)

591 [deaths.html?\\_r=0](http://www.nytimes.com/2015/06/26/world/asia/karachi-pakistan-heat-wave-deaths.html?_r=0)

592

593 Islam, S. U., Rehman, N. and Sheikh, M. M.: Future change in the frequency of warm and cold spells over

594 Pakistan simulated by the PRECIS regional climate model, *Clim. Change*, 94,35-45, doi:10.1007/s10584-

595 009-9557-7, 2009.

596

597 Kalim, U. and Shouting, G. A. O., Moisture Transport over the Arabian Sea Associated with Summer

598 Rainfall over Pakistan in 1994 and 2002. *Advances in Atmospheric Sciences*, 29(3):501–508, 2012.

599

600

601 Leadbetter, M. R., Extremes and local dependence in stationary sequences, *Zeitschrift für*

602 *Wahrscheinlichkeitstheorie und Verwandte Gebiete*, 65, 291-306, doi:10.1007/BF00532484, 1983.

603

604 Loynes, R. M, Extreme Values in Uniformly Mixing Stationary Stochastic Processes, *Ann. Math. Stat.*,

605 36(3), 993–999, doi:10.1214/aoms/1177700071, 1965.

606

607 Luo, P., Apip, He, B., Duan, W., Takara, K. and Nover, D, Impact assessment of rainfall scenarios and land-

608 use change on hydrologic response using synthetic Area IDF curves. *J. Flood Risk Manage.*

609 doi:10.1111/jfr3.12164, 2015.

610

611 Luo, P., He, B., Takara, K., Xiong, Y.E., Nover, D., Duan, W.L., Fukushi, K., Historical assessment of

612 chinese and japanese flood management policies and implications for managing future floods *Environ. Sci.*

613 *Policy*, 48 (2015), pp. 265-277, 2015.

614

615 Lucarini, V., Faranda, D., Wouters, J. and Kuna, T.: Towards a General Theory of Extremes for Observables

616 of Chaotic Dynamical Systems., J. Stat. Phys., 154, 723–750, doi:10.1007/s10955-013-0914-6, 2014.

617 Lucarini, V., Faranda, D., Freitas, A.C.M., Freitas, J.M., Holland, M., Kuna, T., Nicol, M., Todd, M.,  
619 Vaienti, S.: Extremes and Recurrence in Dynamical Systems, John Wiley & Sons Inc, 305, ISBN: 978-1-  
620 118-63219-2  
621 2016.

622 Newell, G. F.: Asymptotic Extremes for  $m$ -Dependent Random Variables, Ann. Math. Stat., 35(3), 1322–  
623 1325, doi:10.1214/aoms/1177703288, 1964.

624 Nogaj, M., Yiou, P., Parey, S., Malek, F. and Naveau, P.: Amplitude and frequency of temperature extremes  
625 over the North Atlantic region, 33, L10801, Geophys. Res. Lett., doi:10.1029/2005GL024251, 2006.

626 IPCC, 2012: *Managing the Risks of Extreme Events and Disasters to Advance Climate Change Adaptation*.  
627 A Special Report of Working Groups I and II of the Intergovernmental Panel on Climate Change [Field,  
628 C.B., V. Barros, T.F. Stocker, D. Qin, D.J. Dokken, K.L. Ebi, M.D. Mastrandrea, K.J. Mach, G.-K. Plattner,  
629 S.K. Allen, M. Tignor, and P.M. Midgley (eds.)]. Cambridge University Press, Cambridge, UK, and New  
630 York, NY, USA, 582 pp.

631 IPCC, Climate Change 2014: Synthesis Report. Contribution of Working Groups I, II and III to the Fifth  
632 Assessment Report of the Intergovernmental Panel on Climate Change [Core Writing Team, R.K. Pachauri  
633 and L.A. Meyer (eds.)]. IPCC, Geneva, Switzerland, 151 pp.2014

634 Pakistan Meteorological Department, Monthly Climatic Normal of Pakistan (1980-2010), Climate Data  
635 Processing Centre (CDPC), Karachi, 2013.

636 Pal, J. S. and Eltahir, E. A. B.: Future temperature in southwest Asia projected to exceed a threshold for  
637 human adaptability, nature climate change, 6, 197-200, doi:10.1038/NCLIMATE2833, 2015.

638 Rasul, G., Mahmood, A., Sadiq, A. and Khan, S. I.: Vulnerability of the Indus Delta to Climate Change in  
639 Pakistan, Pakistan J. Meteorol., 8(16), 2012.

640 Rasul, G., Afzal, M., Zahid, M., Ahsan, S. and Bukhari, A.: Climate Change in Pakistan Focused on Sindh  
641 Province., Technical Report No. PMD-25, 2012.

642 R Development Core Team, R, a language and environment for statistical computing. R Foundation for  
643 Statistical Computing, Vienna, Austria, 2015.

644 Sheridan, S.C., Allen M. J., Changes in the Frequency and Intensity of Extreme Temperature Events and  
645 Human Health Concerns. Current Climate Change Reports 1(3): 155-162, doi:10.1007/s40641-015-0017-3,  
646 2015.

647 Sherwood, S. C. and Huber, M., An adaptability limit to climate change due to heat stress, Proc. Natl. Acad.  
648 Sci. USA 107 9552–5, 2010.

649 Scarrott, C. and Macdonald, A.: A review of extreme value threshold estimation and uncertainty  
650 quantification, Revstat – Stat. J., 10(1), 33–60, 2012.

651 Smith, R. L.: Extreme Value Analysis of Environmental Time Series: An Application to Trend Detection in  
652 Ground-Level Ozone, Stat. Sci., 4(4), 367–377, doi:10.1214/ss/1177012400, 1989.

653 Stull, R.: Wet-bulb temperature from relative humidity and air temperature, J. Appl. Meteorol. Climatol., 50,  
654 2267-2269, doi:10.1175/JAMC-D-11-0143.1, 2011.

655 Tebaldi, C., Hayhoe, K., Arblaster, J. M. and Meehl, G. A.: Going to the extremes: An intercomparison of  
656 model-simulated historical and future changes in extreme events, Clim. Change, 79(3), 185–211,  
657 doi:10.1007/s10584-006-9051-4, 2006.

658 Zahid, M. and Rasul, G.: Rise in Summer Heat Index over Pakistan, Pakistan J. Meteorol., 6(12), 85-96,  
659 2010.

660 Zahid, M. and Rasul, G.: Changing trends of thermal extremes in Pakistan, Clim. Change, 113, 883-896,  
661 doi:10.1007/s10584-011-0390-4, 2012.

662 Zhang, X.B., Zwiers, F.W., Li, G.L., Monte Carlo experiments on the detection of trends in extreme values,  
663 J. Clim. 17, 1945– 1952, 2004.

664  
665  
666  
667  
668  
669  
670  
671  
672  
673  
674  
675  
676  
677  
678  
679  
680  
681  
682  
683  
684  
685

686  
687  
688  
689  
690  
691  
692  
693  
694  
695  
696  
697  
698  
699  
700  
701  
702  
703  
704  
705  
706  
707  
708  
709  
710  
711  
712  
713  
714  
715  
716  
717  
718  
719  
720  
721  
722  
723  
724  
725  
726  
727  
728  
729  
730  
731  
732  
733  
734  
735  
736  
737  
738  
739  
740  
741  
742  
743  
744  
745  
746

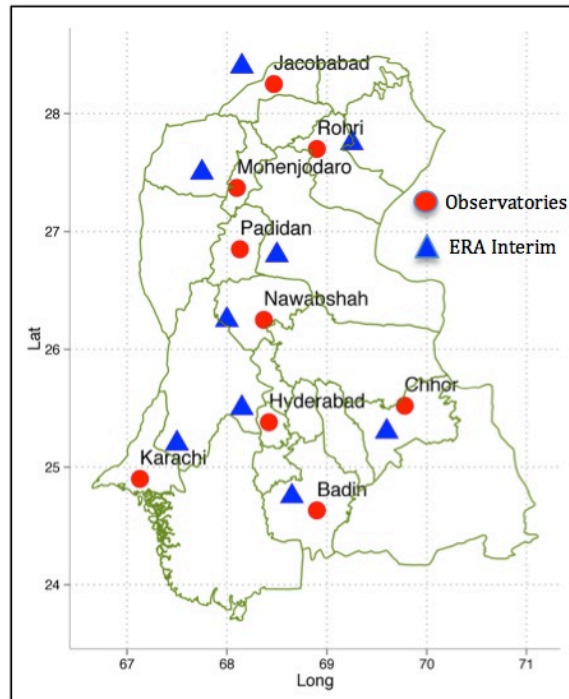


Figure 1: Study Domain (23.5 – 28.5° N , 66.5- 71.1°E)

Table 1. Code, Name, Geographic coordinates and Altitude of the stations.

Code	Name	PMD weather stations			ERA-Interim stations	
		Latitude	Longitude	Altitude (m)	Latitude	Longitude
JCB	Jacobabad	28° 18'N	68° 28'E	55	28 °4'N	68 °15'E
MJD	Mohenjo-daro	27° 22'N	68° 06'E	52.1	27°5'N	67 °75'E
RHI	Rohri	27° 40'N	68° 54'E	66	27°75'N	69 °25'E
PDN	Padidan	26° 51'N	68° 08'E	46	26°8'N	68 °5'E
NWB	Nawabshah	26° 15'N	68° 22'E	37	26°25'N	68 °0'E
HYD	Hyderabad	25° 23'N	68° 25'E	40	25°5'N	68 °15'E
CHR	Chhor	29° 31'N	69° 47' E	5	25°3'N	69 °6'E
KHI	Karachi	24° 54'N	67°08' E	21	25°2'N	67 °5'E
BDN	Badin	24° 38'N	68° 54'E	10	24 °75'N	68 °65'E

747  
748  
749  
750  
751  
752  
753  
754  
755  
756  
757  
758  
759  
760  
761  
762  
763  
764  
765  
766  
767  
768  
769  
770  
771  
772  
773  
774  
775  
776  
777  
778  
779  
780  
781  
782  
783  
784  
785  
786  
787  
788  
789  
790  
791  
792  
793  
794  
795  
796  
797  
798

Table 2. Results of the Kolmogorov-Smirnov Goodness of fit test and Anderson-Darling test between empirical and GPD fits.

Observed $T_{max}$									
Test Statistics	P-value								
	JAC	MJD	RHI	PDN	NWB	HYD	CHR	KHI	BDN
Kolmogorov Smirnov	0.947	0.340	0.996	0.139	0.941	0.385	0.928	0.306	0.666
Anderson Darling	0.553	0.978	0.654	0.857	0.157	0.649	0.233	0.869	0.145
ERA Interim $T_{max}$									
Test Statistics	P-value								
	JAC	MJD	RHI	PDN	NWB	HYD	CHR	KHI	BDN
Kolmogorov Smirnov	0.169	0.125	0.553	0.456	0.322	0.187	0.419	0.456	0.332
Anderson Darling	0.355	0.263	0.165	0.587	0.615	0.398	0.266	0.687	0.425
Bias corrected ERA Interim $T_{max}$									
Test Statistics	P-value								
	JAC	MJD	RHI	PDN	NWB	HYD	CHR	KHI	BDN
Kolmogorov Smirnov	0.452	0.4729	0.197	0.489	0.269	0.137	0.158	0.243	0.312
Anderson Darling	0.352	0.315	0.235	0.270	0.335	0.289	0.216	0.390	0.227
Observed $TW_{max}$									
Test Statistics	P-value								
	JAC	MJD	RHI	PDN	NWB	HYD	CHR	KHI	BDN
Kolmogorov Smirnov	0.981	0.111	0.341	0.226	0.457	0.545	0.441	0.385	0.211
Anderson Darling	0.623	0.745	0.587	0.884	0.199	0.123	0.789	0.669	0.473
ERA Interim $TW_{max}$									
Test Statistics	P-value								
	JAC	MJD	RHI	PDN	NWB	HYD	CHR	KHI	BDN
Kolmogorov Smirnov	0.712	0.564	0.955	0.425	0.258	0.134	0.856	0.497	0.222
Anderson Darling	0.236	0.474	0.516	0.219	0.356	0.117	0.537	0.464	0.613
Bias corrected ERA Interim $TW_{max}$									
Test Statistics	P-value								
	JAC	MJD	RHI	PDN	NWB	HYD	CHR	KHI	BDN
Kolmogorov Smirnov	0.268	0.688	0.127	0.372	0.268	0.229	0.591	0.582	0.478
Anderson Darling	0.373	0.484	0.278	0.432	0.306	0.283	0.365	0.445	0.483

Table 3. Estimated parameters shape  $\xi$ , scale  $\sigma$  and standard error  $\Delta\xi$ ,  $\Delta\sigma$  of all the data sets.

Station observed $T_{max}$									
Estimates	JCB	MJD	RHI	PDN	NWB	HYD	CHR	KHI	BDN
Shape $\xi$	-0.387	-0.255	-0.418	-0.326	-0.332	-0.329	-0.310	-0.222	-0.329
Standard Error $\Delta\xi$	0.031	0.022	0.022	0.021	0.020	0.031	0.037	0.034	0.031
Scale $\sigma$	2.754	2.081	2.351	2.214	2.139	2.228	2.562	2.568	2.228
Standard Error $\Delta\sigma$	0.142	0.104	0.107	0.107	0.103	0.116	0.146	0.144	0.116
ERA Interim $T_{max}$									
Estimates	JCB	MJD	RHI	PDN	NWB	HYD	CHR	KHI	BDN
Shape $\xi$	-0.195	-0.178	-0.207	-0.218	-0.213	-0.338	-0.285	-0.037	-0.251
Standard Error $\Delta\xi$	0.032	0.034	0.034	0.028	0.026	0.031	0.033	0.050	0.037
Scale $\sigma$	1.464	1.323	1.344	1.504	1.563	2.065	1.849	1.330	2.041
Standard Error $\Delta\sigma$	0.079	0.073	0.074	0.078	0.078	0.108	0.094	0.090	0.115
Bias Corrected ERA Interim $T_{max}$									
Estimates	JCB	MJD	RHI	PDN	NWB	HYD	CHR	KHI	BDN
Shape $\xi$	-0.195	-0.178	-0.207	-0.218	-0.213	-0.338	-0.285	-0.037	-0.251
Standard Error $\Delta\xi$	0.032	0.034	0.034	0.028	0.026	0.031	0.033	0.050	0.037
Scale $\sigma$	1.983	1.791	1.820	2.038	2.116	2.798	2.308	1.801	2.763
Standard Error $\Delta\sigma$	0.108	0.100	0.100	0.106	0.106	0.146	0.123	0.122	0.156
Station observed $TW_{max}$									
Estimates	JCB	MJD	RHI	PDN	NWB	HYD	CHR	KHI	BDN
Shape $\xi$	-0.176	-0.186	-0.215	-0.215	-0.216	-0.323	-0.242	-0.219	-0.186
Standard Error $\Delta\xi$	0.038	0.035	0.034	0.044	0.026	0.026	0.034	0.036	0.032
Scale $\sigma$	2.759	2.045	1.960	2.078	1.857	2.372	2.512	2.337	1.903
Standard Error $\Delta\sigma$	0.159	0.114	0.108	0.128	0.093	0.119	0.138	0.132	0.105
ERA Interim $TW_{max}$									
Estimates	JCB	MJD	RHI	PDN	NWB	HYD	CHR	KHI	BDN
Shape $\xi$	-0.089	-0.094	-0.068	-0.125	-0.158	-0.177	-0.090	-0.019	-0.173
Standard Error $\Delta\xi$	0.037	0.029	0.032	0.034	0.031	0.037	0.035	0.035	0.037
Scale $\sigma$	1.287	1.243	1.231	1.440	1.610	1.649	1.3423	0.680	1.788
Standard Error $\Delta\sigma$	0.074	0.066	0.067	0.080	0.087	0.095	0.076	0.039	0.102
Bias Corrected ERA Interim $TW_{max}$									
Estimates	JCB	MJD	RHI	PDN	NWB	HYD	CHR	KHI	BDN
Shape $\xi$	-0.089	-0.094	-0.068	-0.125	-0.158	-0.177	-0.090	-0.019	-0.173
Standard Error $\Delta\xi$	0.037	0.029	0.032	0.034	0.031	0.037	0.035	0.035	0.037
Scale $\sigma$	1.356	1.646	1.758	1.494	1.520	2.052	2.146	1.399	2.152
Standard Error $\Delta\sigma$	0.078	0.087	0.096	0.083	0.082	0.119	0.121	0.081	0.123

849  
850  
851  
852  
853  
854  
855  
856  
857  
858  
859  
860  
861  
862  
863  
864  
865  
866  
867  
868  
869  
870  
871  
872  
873  
874  
875  
876  
877  
878  
879  
880  
881  
882  
883  
884  
885  
886  
887  
888  
889  
890  
891  
892  
893  
894  
895  
896  
897

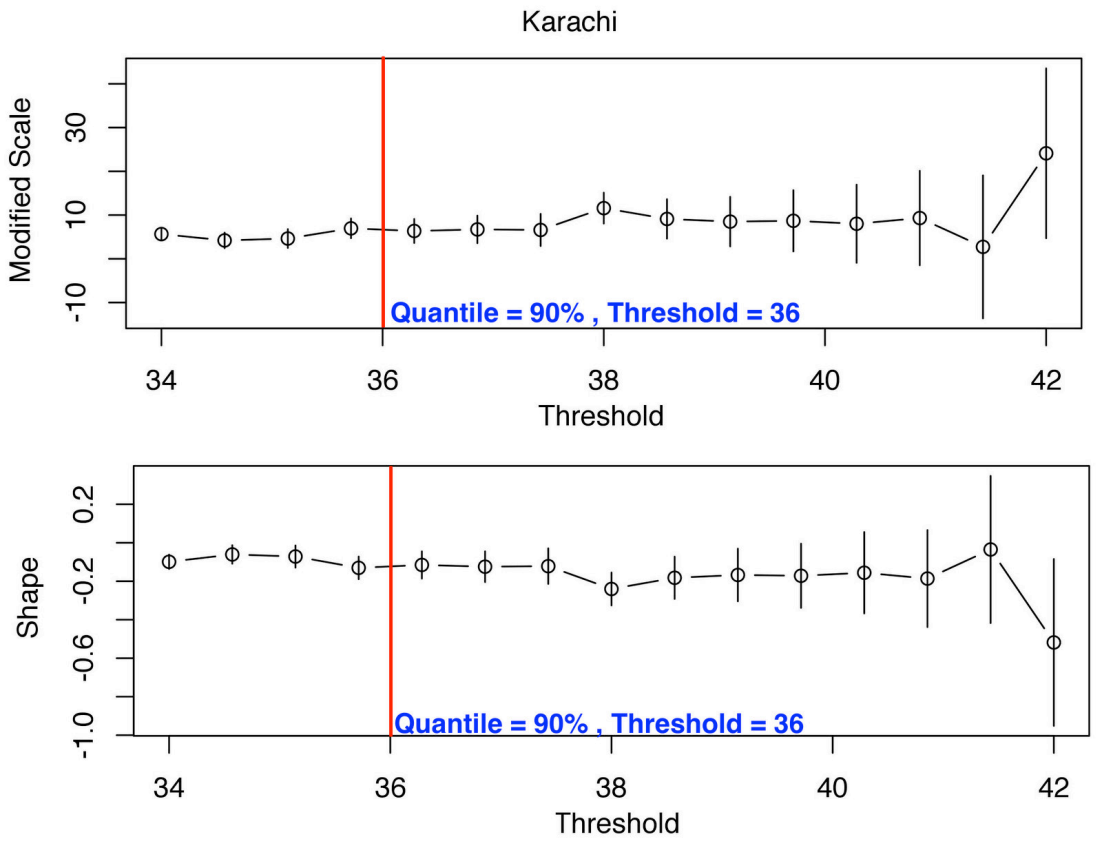


Figure 2. Modified scale ( $\sigma^*$ ) and shape parameter ( $\xi$ ) of the observed  $T_{max}$  ( $^{\circ}\text{C}$ ) Karachi. The red vertical lines represent the selected threshold according to the station quantiles.

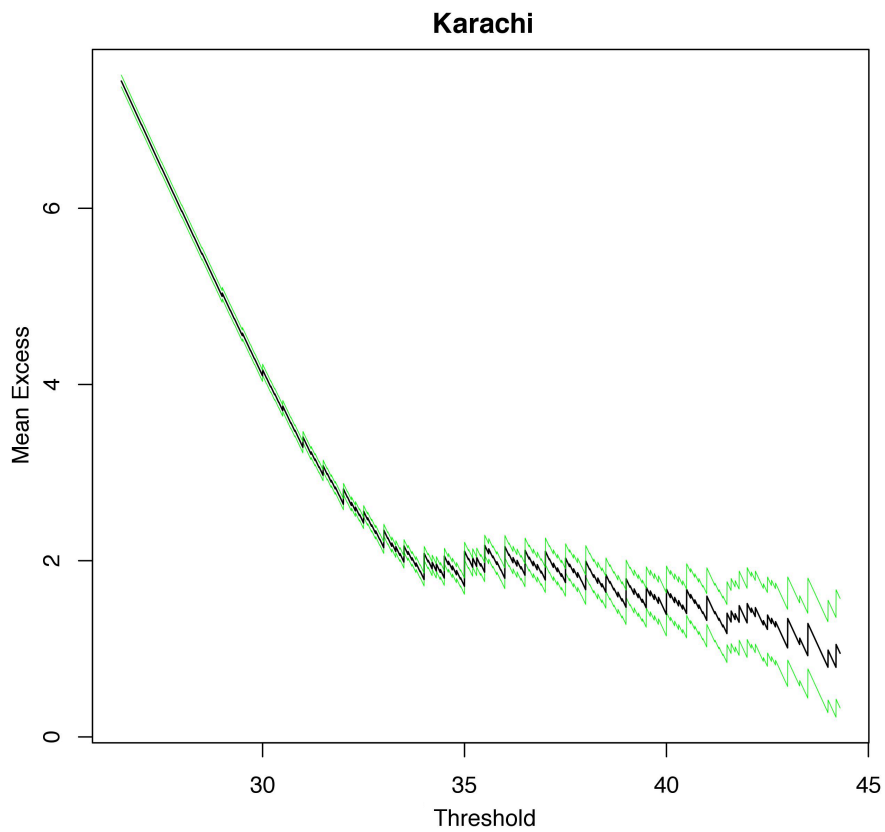


Figure 3. Mean residual life plot of the station observed  $T_{max}$  ( $^{\circ}\text{C}$ ) Karachi.

898  
 899  
 900  
 901  
 902  
 903  
 904  
 905  
 906  
 907  
 908  
 909  
 910  
 911  
 912  
 913  
 914  
 915  
 916  
 917  
 918  
 919  
 920  
 921  
 922  
 923  
 924  
 925  
 926  
 927  
 928  
 929  
 930  
 931  
 932  
 933  
 934  
 935  
 936  
 937  
 938  
 939  
 940  
 941  
 942  
 943  
 944  
 945  
 946  
 947  
 948  
 949  
 950

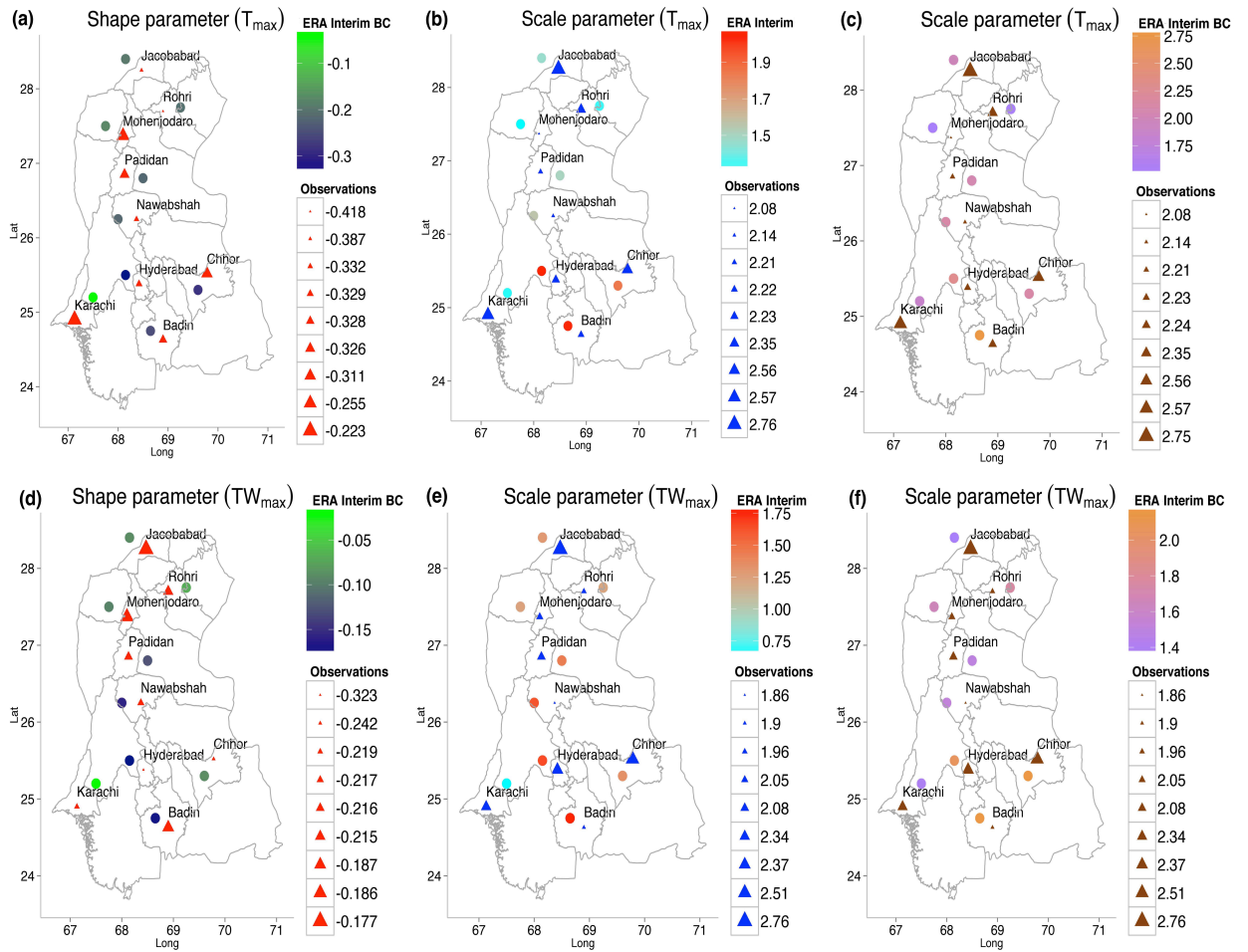


Figure 4. Spatial distribution of the shape parameters  $\xi$  and scale parameters  $\sigma$  of the station observed, ERA Interim, and bias corrected ERA Interim  $T_{max}$  (upper panel) and  $TW_{max}$  (lower panel) degree Celsius.



951  
 952  
 953  
 954  
 955  
 956  
 957  
 958  
 959  
 960  
 961  
 962  
 963  
 964  
 965  
 966  
 967  
 968  
 969  
 970  
 971  
 972  
 973  
 974  
 975  
 976  
 977  
 978  
 979  
 980  
 981  
 982  
 983  
 984  
 985  
 986  
 987  
 988  
 989  
 990  
 991  
 992  
 993  
 994  
 995  
 996  
 997  
 998  
 999  
 1000  
 1001  
 1002  
 1003  
 1004  
 1005  
 1006  
 1007  
 1008  
 1009  
 1010

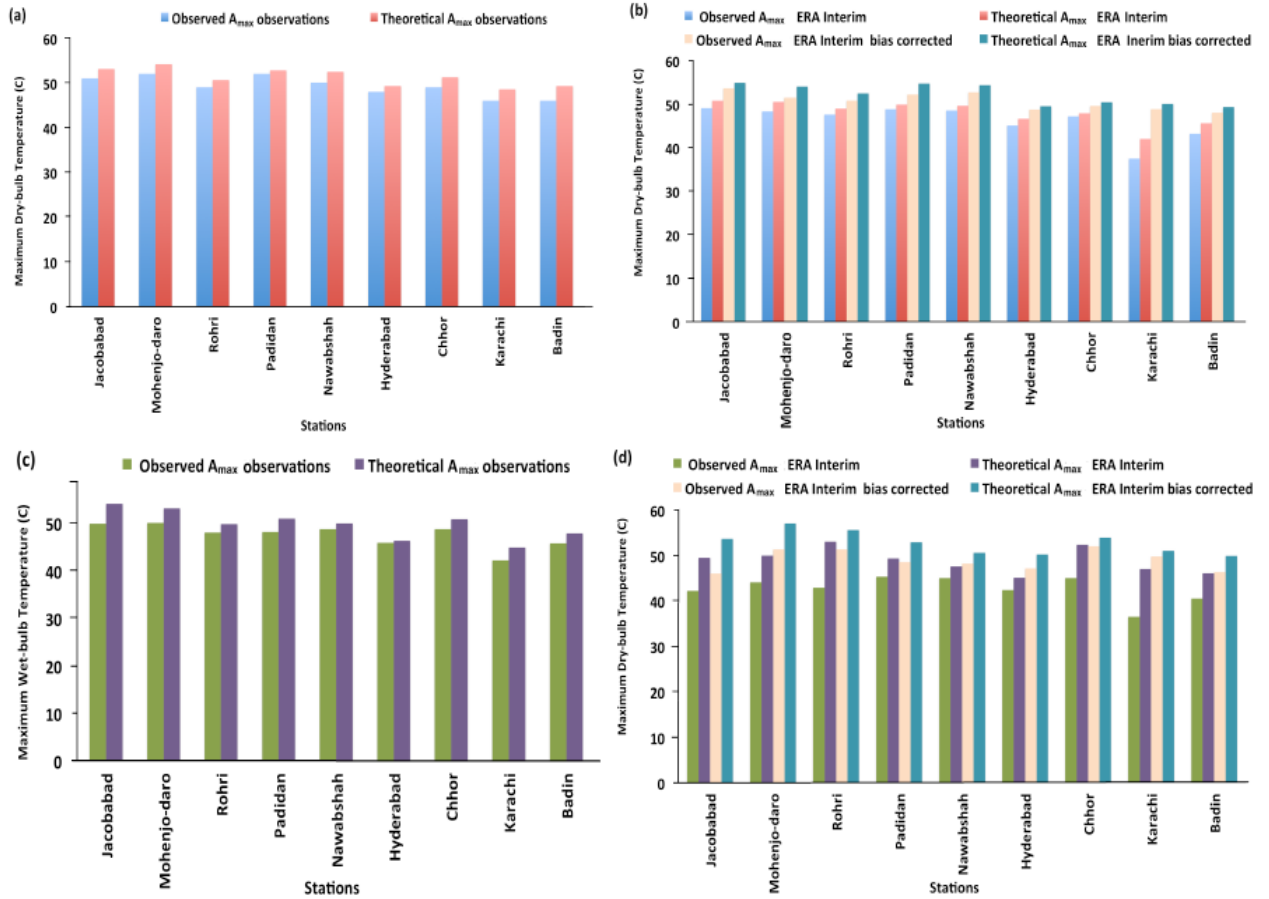


Figure 5. Absolute maxima  $A_{max}$  in degree Celsius (a) station observed  $T_{max}$  (b) ERA Interim and bias corrected ERA Interim  $T_{max}$  (c) station observed  $TW_{max}$  (d) ERA Interim and bias corrected ERA Interim  $TW_{max}$ .

1011  
 1012  
 1013  
 1014  
 1015  
 1016  
 1017  
 1018  
 1019  
 1020  
 1021  
 1022  
 1023  
 1024  
 1025  
 1026  
 1027  
 1028  
 1029  
 1030  
 1031  
 1032  
 1033  
 1034  
 1035  
 1036  
 1037  
 1038  
 1039  
 1040  
 1041  
 1042  
 1043  
 1044  
 1045  
 1046  
 1047  
 1048  
 1049  
 1050  
 1051  
 1052  
 1053  
 1054  
 1055  
 1056  
 1057  
 1058  
 1059  
 1060  
 1061  
 1062  
 1063  
 1064  
 1065

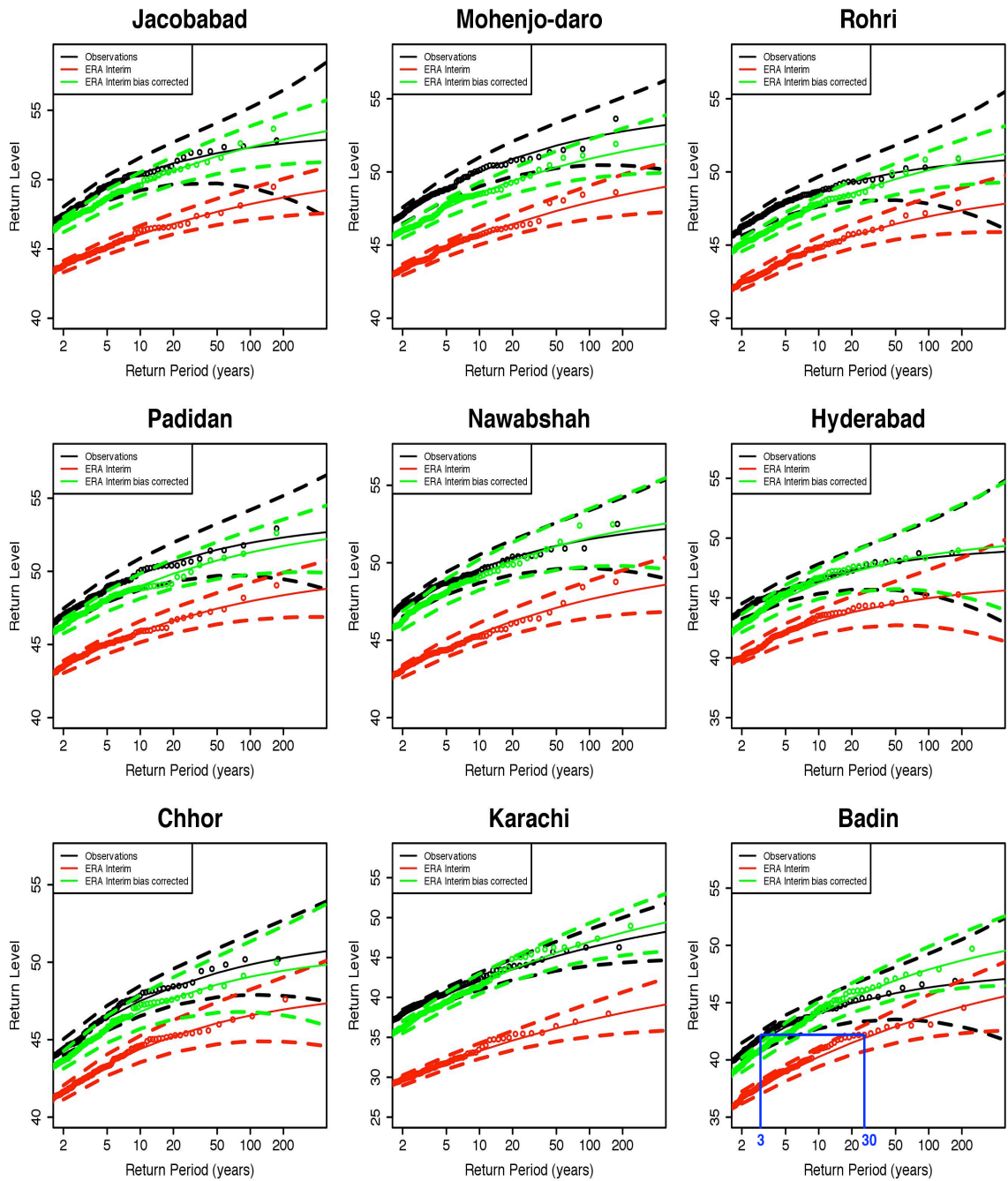


Figure 6. Return level plots of the station observed  $T_{max}$  (black) , ERA Interim  $T_{max}$  (red), and bias corrected ERA Interim  $T_{max}$  (green) in degree Celsius. The blue line is to show a difference in the observed and ERA Interim RLs.

1066  
 1067  
 1068  
 1069  
 1070  
 1071  
 1072  
 1073  
 1074  
 1075  
 1076  
 1077  
 1078  
 1079  
 1080  
 1081  
 1082  
 1083  
 1084  
 1085  
 1086  
 1087  
 1088  
 1089  
 1090  
 1091  
 1092  
 1093  
 1094  
 1095  
 1096  
 1097  
 1098  
 1099  
 1100  
 1101  
 1102  
 1103  
 1104  
 1105  
 1106  
 1107  
 1108  
 1109  
 1110  
 1111  
 1112  
 1113  
 1114

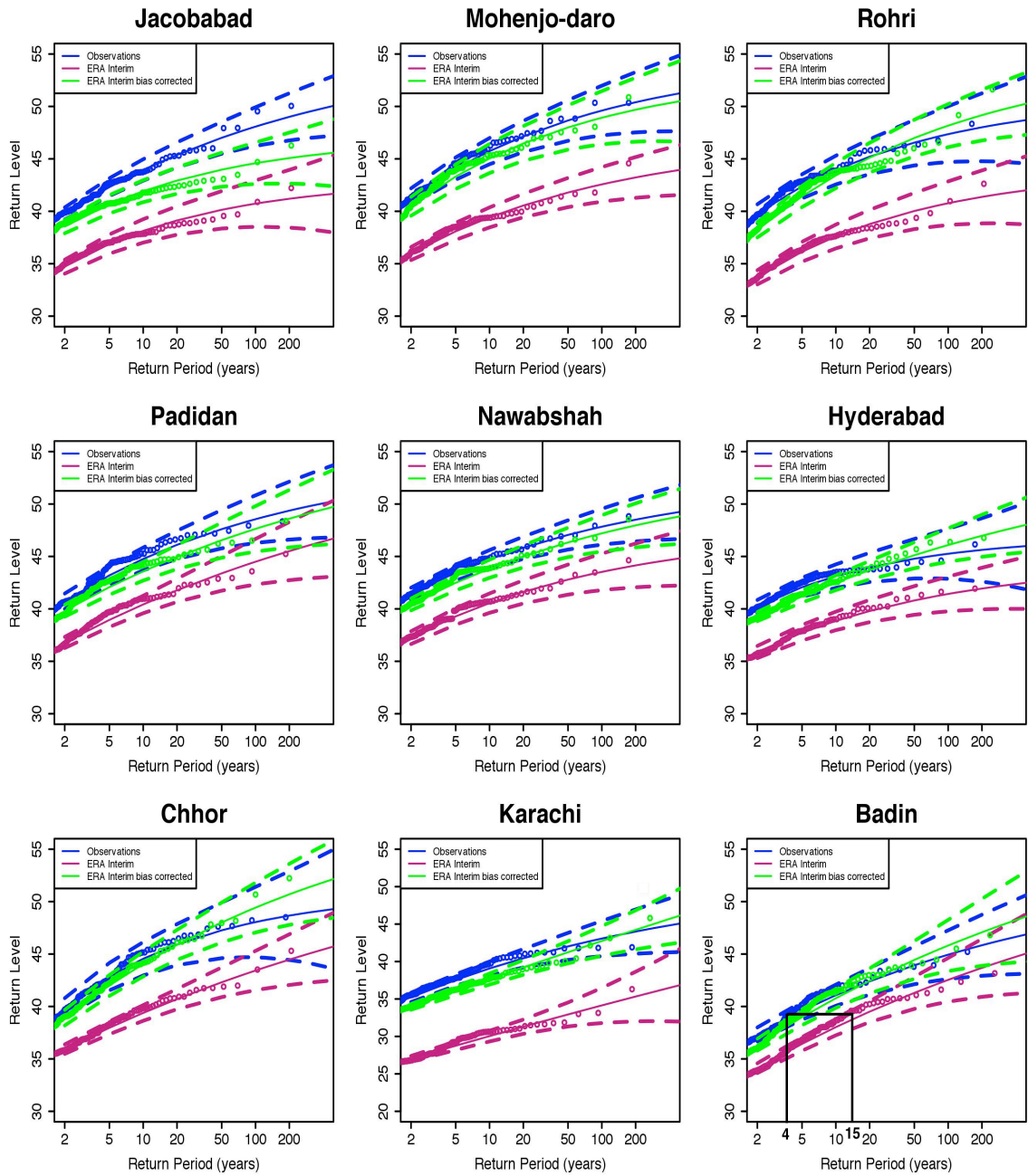


Figure 7. Return level plots of the station observed  $T_{max}$  (blue), ERA Interim  $T_{max}$  (pink), and bias corrected ERA Interim  $T_{max}$  (green) in degree Celsius. The black line is to show a difference in the observed and ERA Interim RLs.

1115  
 1116  
 1117  
 1118  
 1119  
 1120  
 1121  
 1122  
 1123  
 1124  
 1125  
 1126  
 1127  
 1128  
 1129  
 1130  
 1131  
 1132  
 1133  
 1134  
 1135  
 1136  
 1137  
 1138  
 1139  
 1140  
 1141  
 1142  
 1143  
 1144  
 1145  
 1146  
 1147  
 1148  
 1149  
 1150  
 1151  
 1152  
 1153  
 1154  
 1155  
 1156  
 1157  
 1158  
 1159  
 1160  
 1161  
 1162  
 1163  
 1164  
 1165  
 1166

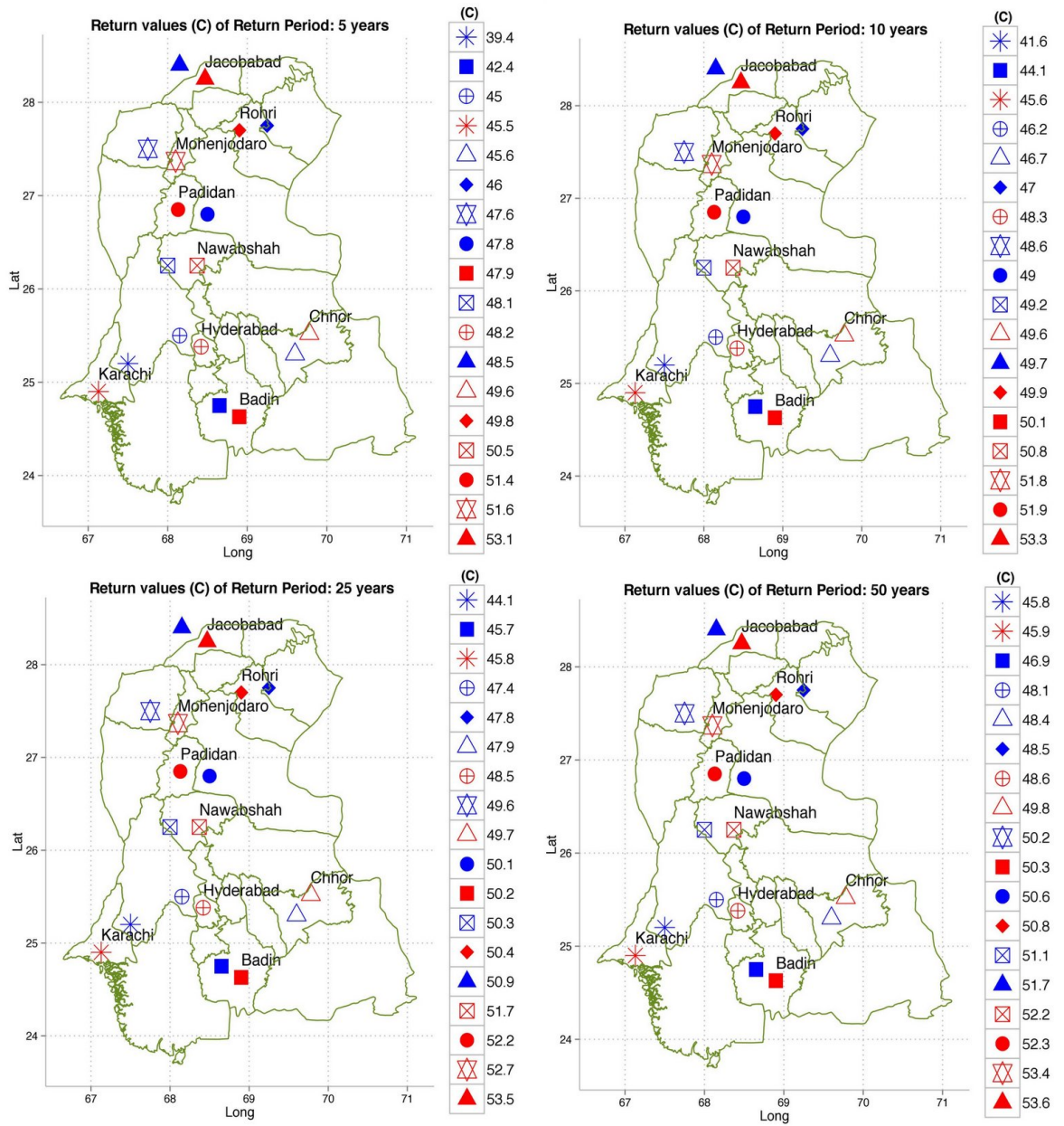


Figure 8. Spatial distribution of the station observed  $T_{max}$  (red) and bias corrected ERA Interim  $T_{max}$  (blue) return levels in degree Celsius corresponding to return periods of 5, 10, 25 and 50 years in southern Pakistan.



1167  
 1168  
 1169  
 1170  
 1171  
 1172  
 1173  
 1174  
 1175  
 1176  
 1177  
 1178  
 1179  
 1180  
 1181  
 1182  
 1183  
 1184  
 1185  
 1186  
 1187  
 1188  
 1189  
 1190  
 1191  
 1192  
 1193  
 1194  
 1195  
 1196  
 1197  
 1198  
 1199  
 1200  
 1201  
 1202  
 1203  
 1204  
 1205  
 1206  
 1207  
 1208  
 1209  
 1210  
 1211  
 1212  
 1213  
 1214  
 1215  
 1216  
 1217

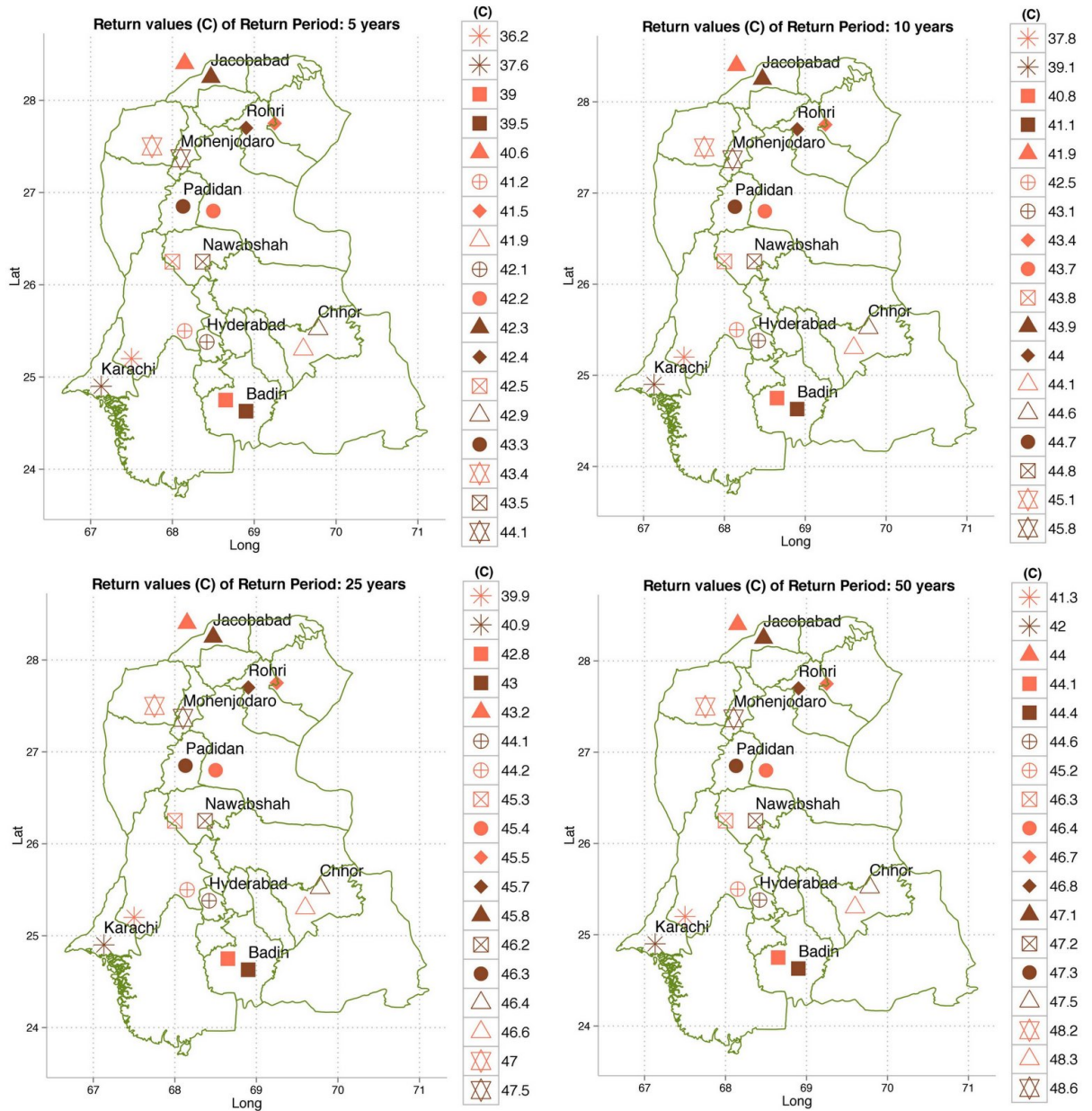


Figure 9. Spatial distribution of the station observed  $TW_{max}$  (brown) and bias corrected ERA Interim  $TW_{max}$  (orange) return levels in degree Celsius corresponding to return periods of 5, 10, 25 and 50 years in southern Pakistan.